Full Paper: Monte Carlo simulations have been performed for realistically dense liquids of model trimers consisting of rigid cores connected by virtual bonds representing semiflexible spacers. The conformational characteristics of the trimers are approximately regulated in two cases to mimic $(CH_2)_n$ spacers with n odd or even. All simulated systems undergo reversible isotropic–nematic phase transitions at well defined temperatures, showing odd–even oscillations in good agreement with experiments. The transitions are coupled with a conformational selection favoring extended conformations in the nematic liquids. The odd–even oscillations and the conformational distribution in the nematic liquids are fully explained on the basis of the intrinsic conformational characteristics of the model trimers.

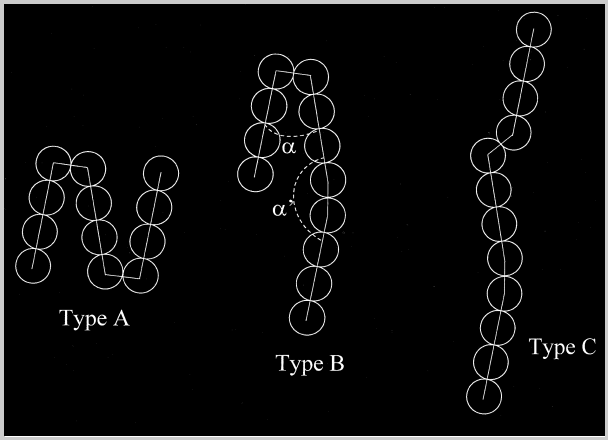

Conformations of Type A ($\alpha < 60^\circ$, $\alpha' < 60^\circ$; see the text), Type B ($\alpha < 60^\circ$, $\alpha' > 120^\circ$ or vice versa) and Type C ($\alpha > 120^\circ$, $\alpha' > 120^\circ$).

Order–Disorder Transitions in Model Liquids of Mesogenic Trimers

Michele Vacatello

Dipartimento di Chimica, Università di Napoli, Via Cinthia – I-80126 Napoli, Italy
E-mail: vacatello@chemistry.unina.it; Fax: (+39)-81-674325

Keywords: liquid-crystalline polymers (LCP); Monte Carlo simulation; order-disorder transitions

Introduction

Segmented-chain mesogenic polymers, i.e., polymers comprised of alternating semiflexible segments and sufficiently elongated conformationally rigid groups, give rise on melting to mesophases in which the peculiar properties of polymeric materials are coupled with the long-range orientational order characteristic of liquid crystals. Hence, they have been the subject of intense investigations in recent years, both theoretically and experimentally.[1–35] A distinctive feature of this class of polymers shows that relevant properties such as the isotropization temperature, enthalpy and entropy exhibit more or less pronounced odd–even oscillations on varying the semiflexible spacer length, the entity of the oscillations decreasing with increasing length and flexibility of the spacers. This clearly indicates that the spacers are far from behaving as a bound solvent, unless they are very long and flexible. On the contrary, they play, in most cases, an active role, not only by conveying information on the mutual orientation between consecutive rigid groups, but also by adapting their own orientation and conformation to the anisotropy of the environment. This behavior creates a severe theoretical problem, given the difficulty of incorporating into a single analytical treatment the cooperative effects of the anisometry of the rigid groups and the translational, orientational and conformational constraints deriving from the presence of the semiflexible spacers.[2–11]

In order to expand our knowledge of the essential aspects of the problem, this paper presents the results of Monte Carlo simulation studies of dense systems of model trimers constituted by rigid groups connected by semiflexible spacers. The choice of modeling trimers, rather than longer oligomers or polymers, is mainly due to the computational convenience, but it is also based on the experimental observation that dimers and trimers exhibit most of the relevant properties of the corresponding polymers.[1,3] Both Molecular Dynamics and Monte Carlo methods have been utilized in the last two decades to perform computer experiments on a variety of model

 © WILEY-VCH Verlag GmbH, 69469 Weinheim 2002 1022-1344/2002/0506–0501$17.50+.50/0

liquid-crystal systems, ranging from fluids of hard bodies such as spherocylinders, ellipsoids or platelets,[18–23] to soft ellipsoids[24–26] modeled by use of the Gay–Berne potential,[27] to more realistic simulations in which the individual atoms and their mutual interactions are explicitly taken into account.[28–32] Most of these studies have examined relatively small systems, usually consisting of a periodically repeating base cell containing less than 500 molecules in the case of hard or soft bodies,[18–21, 24, 25] or less than 100 molecules in the case of realistic simulations.[28–31] Larger systems (up to 8000 molecules for hard bodies) have been simulated in the last few years.[22, 23, 26, 32] However, realistically dense liquids of segmented-chain trimers or oligomers have been not simulated up to now.

Recently, large-scale Monte Carlo simulations have been utilized to investigate the thermal behavior of model liquids of rigid anisometric molecules at a density comparable with the density of mesogenic groups in liquid-crystalline substances.[33–35] Though idealized with respect to the variety and complexity of real systems, these models take into account all those key factors possibly responsible for the onset of nematic order. The large-scale simulations of refs.[33–35] have enabled to observe reversible nematic–isotropic phase transitions, in the sense that the same phase is normally obtained both on heating more ordered systems equilibrated at lower temperatures and on cooling more disordered systems obtained at higher temperatures (metastable ordered phases are observed in a few cases at temperatures very close to the transition point). It has been also shown that the results do not depend on the size of the base cell utilized in the simulations, provided that this cell is much larger than those usually studied in the literature.

Segmented-chain mesogenic trimers are simulated here using a model and a set of parameters practically coincident with those of the system of rigid anisometric molecules studied in ref.[35] In practice, the trimer molecules are constituted by three of the latter molecules connected in sequence. However, in order to investigate the principal factors responsible for the observed behavior of segmented-chain oligomers and polymers, four separate simulations are performed for trimers with different conformational characteristics. In two of these simulations, the conformational characteristics of the model trimers are approximately regulated to mimic the presence of odd or even poly(methylene) spacers, respectively. Some results have been already published in the form of a preprint.[36]

Models and Methods

The Simulated Systems

The anisometric molecules simulated in ref.[35] (system RC) consist of four isodiametric units rigidly connected in linear sequences by links of length σ. The trimers are simply modeled in the present work by connecting in sequence the end units of three such anisometric molecules by links of the same length, σ (see Figure 1, upper part). All interactions among the rigid cores are treated as in ref.[35] That is, the isodiametric units interact through a shifted 12-6 Lennard-Jones potential $E_{nb} = \varepsilon[(\sigma/r)^{12} - 2(\sigma/r)^6 + 1]$, with r the distance between the interacting units and $\varepsilon = 416$ J mol^{-1}, truncated at the distance σ in such a way that only repulsive interactions are included; the minimum distance allowed between units is $r_{min} = 0.75\ \sigma$. Attractive anisotropic interactions are modeled in the mean-field form $E_{mf} = -A\ s_{rc}\ (3\cos^2\theta - 1)/2$, where θ is the angle between a rigid core and the nematic director (assumed coincident with the z axis in these calculations), $s_{rc} = (3\ \langle\cos^2\theta\rangle - 1)/2$ is the order parameter of the rigid cores and $A = 7.6$ kJ mol^{-1} (this value of A was selected in ref.[35] in order to have the nematic-isotropic transition for system RC near room temperature). The adoption of a mean-field approximation, in a form coincident with that utilized in popular theories of liquid crystals,[37–39] makes the calculations simpler and much faster, and allows one to compare the results with theoretical predictions. Although the thermal behavior of the simulated systems is obviously governed in part by the mean field itself, previous calculations indicate that the model is quite sensitive to relatively small changes of molecular shape, and that the simulated properties show trends in good agreement with theories[35] (as well as with common sense). As in ref.,[35] the systems simulated here consist of three-dimensionally periodic cubic cells with edges 40σ containing 10668 rigid groups (3556 trimer molecules), giving a density of rigid cores comparable with the density of rigid cores in most real nematics (i.e., 2/3 of the volume is occupied by the rigid cores, while the rest of the space is considered to be filled by flexible end groups in system RC, and by end groups and spacers in the trimers; these groups are assumed to behave only as a diluent as far as the repulsive and attractive interactions among rigid cores are concerned).

Conformational Energy of the Trimers

The conformation of a model trimer molecule is fully specified by four angles between consecutive links (τ_1, τ_2, τ_3, τ_4 in Figure 1) and three dihedral angles (φ_1, φ_2 and φ^* in Figure 1, upper part). Therefore, the total energy of the system is evaluated by adding conformational terms E_τ and E_φ, depending on the values assumed by the angles τ_i and φ_i in each trimer molecule, respectively. In two cases, these terms are roughly regulated to model the presence of odd or even poly(methylene) spacers at the two junctions. The torsion angle φ^* is assumed to be totally free.

The conformational distribution of typical spacers has been investigated in the past (see, for instance, the RIS

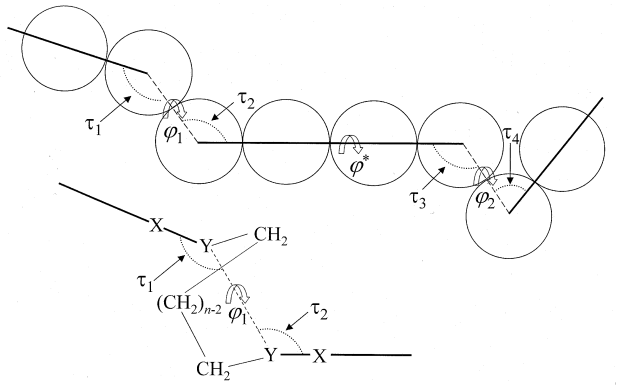

Figure 1. Model trimers and definition of the angles τ_i, φ_i and φ^*.

calculations of Abe[2] and of Yoon and Bruckner[4]). Unfortunately, the results presented in the literature cannot be directly translated in terms of the energy contributions required for the present simulations. In order to model a simple case of trimers containing poly(methylene) spacers, the angles τ_i and φ_i are considered here equivalent to the corresponding angles in the lower part of Figure 1, where the X–Y bonds are part of the rigid cores and are aligned with their long axes, while the broken line represents a virtual bond connecting the terminal atoms of consecutive rigid cores. Distributions of τ_i and φ_i for $(CH_2)_n$ spacers have been obtained by assuming that the conformational characteristics of X—Y—CH_2—CH_2 and of Y—CH_2—CH_2—CH_2 bonds are coincident with those of poly(methylene) bonds. Consequences and limitations of this procedure are discussed later in this subsection. Monte Carlo simulations of unperturbed CH_3—CH_2—$(CH_2)_n$—CH_2—CH_3 molecules have been performed at the united atom level, utilizing the force field described in ref.[40] with the addition of a harmonic bending energy contribution for the C—C—C bond angles (bending constant 958 kJ · mol^{-1} · rad^{-2}, minimum energy angle 111°; see ref.[41]). Calculations have been performed at 320 K by averaging over a very large number of conformations for each value of n.

Figure 2 shows that the resulting distributions of τ ($=\tau_i$) are characterized by several maxima and minima for the first few terms of the series (Figure 2a). On the other hand, in the more interesting range $4 < n < 10$ (Figure 2b), the distributions are characterized by a single broad maximum approximately centered at 120°. Of course, this maximum tends to shift toward 90° with increasing n. A distribution with a single broad maximum can be easily obtained in the model trimers by placing $E_\tau = (k_\tau/2)(\tau-\pi)^2$. In particular, when k_τ is 1.0–1.5 kJ · mol^{-1} · rad^{-2}, the maximum is predicted to be around 120°. However, even taking into account that angles smaller than 50° lead to distances between core units less than r_{min} and are forbidden in the model, the population evaluated with k_τ = 1.0–1.5 kJ · mol^{-1} · rad^{-2} is higher than in Figure 3 for τ between

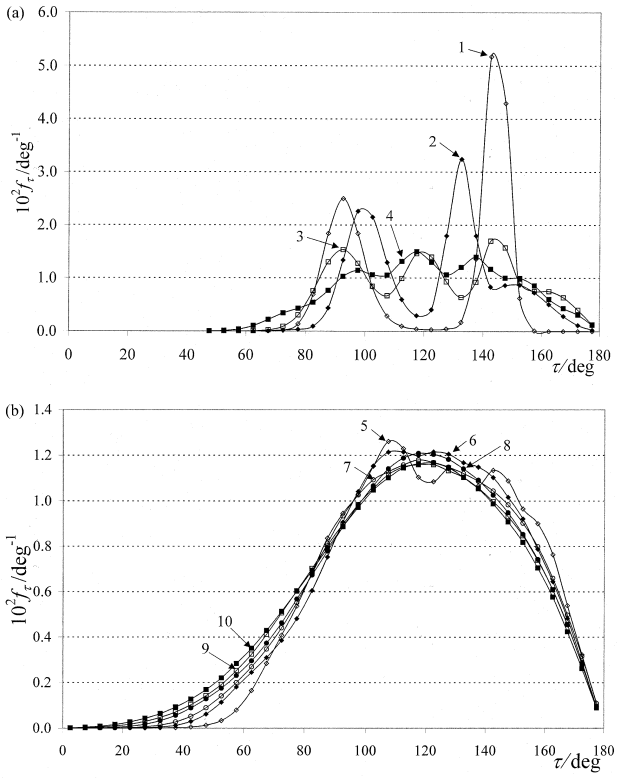

Figure 2. Distribution of the angles τ_i (see Figure 1) for $(CH_2)_n$ spacers with n = 1–4 (2a) and n = 5–10 (2b).

50° and 100°. Increasing k_τ to 2.0–3.0 kJ · mol^{-1} · rad^{-2} shifts the location of the maximum near 130°, but reduces the population at lower angles in such a way that when k_τ = 2.6 kJ · mol^{-1} · rad^{-2} the predicted distribution is much closer to that shown in Figure 2b. Therefore, the trimers have been simulated with $E_\tau = (k_\tau/2)(\tau-\pi)^2$ and k_τ = 2.6 kJ · mol^{-1} · rad^{-2}.

The distributions of the absolute value of φ ($=\varphi_i$) obtained for various values of n are shown in Figure 3. It is immediately clear that, for $n > 4$, even members of the series show maxima at 50–60° and at 180°, separated by two intervening minima at 0° and at 110–120°, while the behavior of odd members is exactly the opposite. Of course, the intensity of all these features decreases with increasing n. Energies E_φ to be used in the trimer simulations have been obtained by cubic spline interpolation of the data plotted in Figure 3b, after reducing them to the form $E_\varphi = -RT\ln(f_\varphi/f_{max})$, where T = 320 K and f_{max} is the maximum value of f_φ for the given value of n.

The four systems simulated in this work have exactly the same composition, and differ only for the conformational properties of the trimers. System T_0 is constituted by trimer molecules in which the angles τ_i and φ_i are totally unrestricted, while in system T_b the angles τ_i are restricted by E_τ and the torsion angles φ_i are unrestricted. The energy contribution E_φ, deduced as before for poly(methylene) spacers with n = 5 and n = 6, is applied together with E_τ to systems T_5 and T_6, respectively.

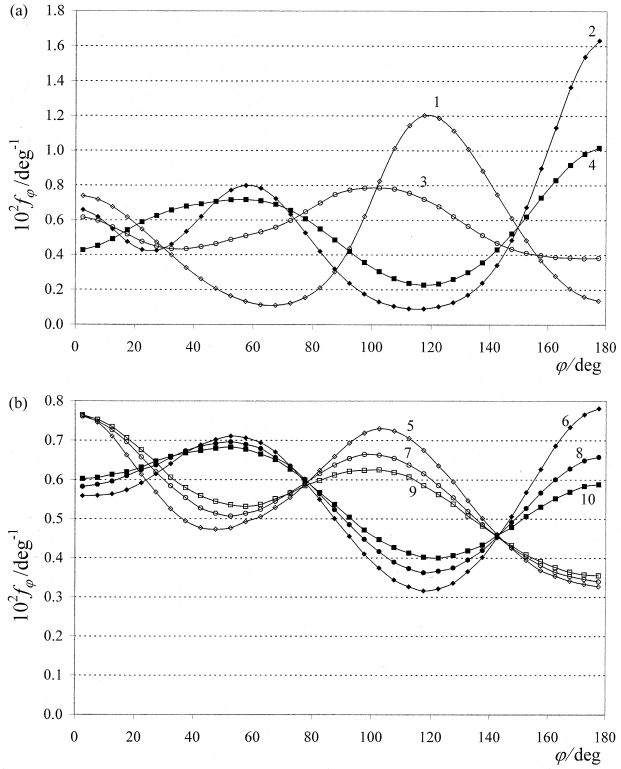

Figure 3. Distribution of the torsion angles φ_i (absolute values; see Figure 1) for $(CH_2)_n$ spacers with $n = 1–4$ (3 a) and $n = 5–10$ (3 b).

One has to remark that the present calculations are not meant to simulate the behavior of specific classes of trimers or polymers. On one hand, the rigid cores are modeled at a coarse grained level and the anisotropic part of their attractive interactions is treated in a simple mean-field approximation. On the other hand, the model trimers in systems T_5 and T_6 are such that the X—Y bonds (Figure 1) are aligned with the rigid cores, and all bonds in the spacers (including the connection to the rigid cores) are considered to have conformational properties identical to poly(methylene) bonds. Therefore, the simulated systems are to be considered as simple illustrative models allowing to highlight the role of the semiflexible spacers and to study origin and nature of a number of interesting aspects of the behavior of segmented-chain mesogenic polymers. Also, utilizing E_τ and E_φ in the form given above totally neglects correlations between the angles τ_i and the torsion angles φ_i. Correlations of this kind are present in poly(methylene) spacers, in the sense that different distributions of τ are obtained for various values of φ. They have not been included here because their presence would be confusing and would obfuscate in part the effects discussed in the next section. However, they should be investigated and taken into account in more realistic simulations. When considering real polymers with poly(methylene) spacers, the results shown in the next section may be roughly approximate in some cases, but are totally inadequate in many others. For instance, in polyesters like those of the two series [OC—Ph—...—Ph—COO$(CH_2)_m$—O—] and [O—Ph—...—Ph—OOC$(CH_2)_m$—CO—], it is easy to identify the X–Y bonds with the Ph–CO bonds or with the Ph—O bonds, respectively (provided that these bonds can be considered collinear with the rigid groups). However, approximating the conformational properties of the ester bonds and of bonds in their neighborhood with those of —CH_2—CH_2— bonds is plainly wrong, as confirmed by the experimental finding that reversing the direction of the ester linkages substantially modifies the behavior of mesogenic polyesters.[42, 43] In conclusion, the behavior of real polymers can be only simulated by obtaining expressions for E_τ and E_φ appropriate for the particular systems under study and by taking into account correlations between τ_i and φ_i. Of course, all other parameters of the model (density, value of the mean-field parameter A, etc.) should be properly regulated.

Calculations

The initial configuration of the systems is generated with rigid groups oriented along the z axis, with all τ angles equal to 135° and with all φ angles equal to 180°. This configuration is otherwise random, with the further condition that two non-bonded units do not approach at a distance smaller than r_{min}. The simulated systems are equilibrated in the canonical (*NVT*) ensemble at various temperatures by Monte Carlo (MC) methods using trial moves consisting of a combination of translations, rigid rotations and conformational changes. Trial moves are performed by translating the center of mass of the selected molecule at random inside a sphere of diameter 0.4σ, while also rotating the whole molecule around a random vector of a random angle in the range [–20°, 20°]. Following this, the molecular conformation is changed by rotating rigid cores and intermediate links around independent random vectors of random angles in the range [–20°, 20°]. The trial configuration is then immediately rejected if distances less than r_{min} occur. Otherwise, the total energy change is evaluated and the new configuration is accepted or rejected according to the outcome of a standard Boltzmann test. Since the overall order parameter of the rigid cores changes when attempting a MC move, the value of E_{mf} after the move is evaluated with $s'_{rc} = s_{rc} + 3\Sigma(\cos^2\theta'_i - \cos^2\theta_i)/2N$, where the primed symbols refer to quantities after the move, N is the total number of rigid cores and the sum is over the three rigid cores that changed their orientation. When a move is accepted, s_{rc} is updated accordingly. A MC cycle is defined to consist of 10^8 attempted moves, approximately 1.5% of which are accepted. Each simulation has been separately performed on a dedicated PC, one MC cycle taking approximately 80 min on computers equipped with Athlon 800 MHz processors.

Although the fraction of accepted moves is relatively small, the methods utilized for equilibrating the systems at various temperatures and for sampling the configuration space are quite efficient. In particular, the translational and orientational mobilities are large enough for adjacent molecules to exchange their position very frequently in each calculation, while also inverting several times their orientation with respect to the z axis. For instance, the internal rigid cores of the trimers in the orientationally ordered phase stable for system T_5 at 300 K (see next section) are found to reverse their direction along the z axis every 10 cycles on the average. On the other hand, the mean-square displacement of the centers of mass of these internal rigid cores is as high as 2.5 σ^2/cycle in the isotropic phase of system T_6 at 335 K. It is even higher (3.6 σ^2/cycle) in the ordered phase stable at 330 K for this system, since the apparent diffusivity perpendicular to the director is nearly unchanged going from the isotropic to the ordered phase, while the diffusivity parallel to the director is much higher in the latter case.

Results and Discussion

Thermal Behavior of the Model Systems

For each system of trimers, several calculations have been performed at various temperatures and with various starting configurations. Figure 4 plots, as an example, the change of the orientational order parameter of the rigid cores as a function of Monte Carlo cycles in the calculations performed for system T_5. From left to right:

a) Starting point: the initial system with $s_{rc} = 1$. At T = 320 K, the order parameter rapidly decreases, reaching a value approximately 0.25 in 30 cycles only.
b) Starting point: a configuration with $s_{rc} = 0.33$ obtained after 26 cycles at 320 K. At T = 310 K, the system continues to evolve toward the random isotropic phase, while at T = 300 K the order parameter increases and appears to level off at $s_{rc} = 0.53$, suggesting that the anisotropic–isotropic transition temperature be located between 300 K and 310 K.
c) Starting point: a system with $s_{rc} = 0.52$ obtained at 300 K. At T = 295 K and at T = 280 K the order parameter increases and levels off at $s_{rc} = 0.56$ and $s_{rc} = 0.64$, respectively. On the contrary, at T = 305 K the order parameter decreases and the system changes to the isotropic phase. It is concluded that the anisotropic–isotropic transition temperature is located in the range 300–305 K.
d) Starting point: a system with $s_{rc} = 0.54$ obtained at 295 K. Cooling at T = 290 K, the order parameter increases and levels off at $s_{rc} = 0.59$.
e) Starting point: a system with $s_{rc} = 0.64$ obtained at 280 K. Cooling at T = 270 K, the order parameter increases up to at $s_{rc} = 0.68$.

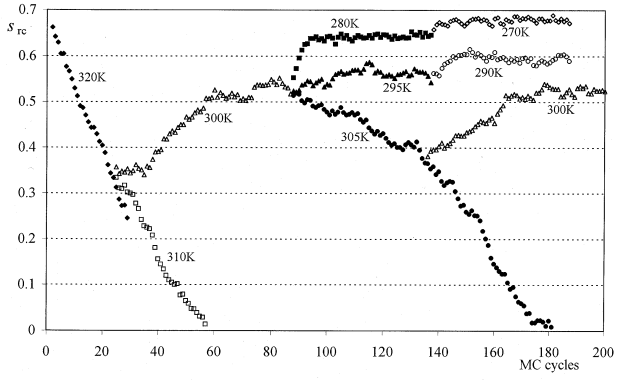

Figure 4. Behavior of the order parameter of the rigid cores (s_{rc}) as a function of Monte Carlo cycles in the calculations performed for system T_5.

f) Starting point: a system with $s_{rc} = 0.37$ obtained during the 305 K run. At 300 K, the order parameter increases and levels off at the same value (0.53) obtained in b) at the same temperature.

Similar calculations have been performed for all systems investigated. The results, summarized in Table 1, indicate that the transition from the anisotropic to the isotropic phase takes place for the various systems in the following ranges: 300–305 K (system T_0), 320–325 K (system T_b), 300–305 K (system T_5), 330–335 K (system T_6). The ordered configuration with $s_{rc} = 0.48$ obtained at 305 K in run 4 for system T_0 and the ordered configuration with $s_{rc} = 0.52$ obtained at 325 K in run 5 for system T_b are probably metastable, since the isotropic phase is obtained at the same temperatures when starting from less ordered configurations with $s_{rc} \approx 0.33$ (the theoretical grounds of this method are discussed in ref.[33, 34]). No metastable configurations are observed for systems T_5 and T_6. It has been checked that the distribution of the centers of mass of the rigid cores along the z axis does not show evidence of long-range positional order for all systems at all temperatures investigated. Therefore, the ordered phase can be classified in all cases as nematic. Note that the transition temperatures are mainly regulated by the density and by the mean-field parameter A. In order to model real systems, the density should be set at the experimental value for the various members of the series, and A should be adjusted such to bring the transition temperature in the experimental range. Of course, changing these parameters may also change the order parameters at the transition points and the exact values of other properties. On the other hand, the density and the value of A used here (chosen such to allow a better comparison with previous calculations) are close enough to experimental conditions to believe that the general trends would be not substantially modified in this process.

The nematic–isotropic transition temperatures of systems T_0 and T_5 are seen to be coincident with that observed in ref.[35] for system RC (the reference system of

Table 1. Summary of the calculations performed. All entries are in the form $T_1(s_{rc,1})–T_2(s_{rc,2})$, meaning that a system with order parameter of the rigid cores $s_{rc,1}$ obtained at temperature T_1 was heated or cooled at temperature T_2, $s_{rc,2}$ being the average order parameter of the rigid cores obtained at T_2 (In = initial system with $s_{rc} = 1$; iso = isotropic). Some of the calculations tending to the isotropic phase were halted before reaching the isotropic limit.

	System T_0	System T_b	System T_5	System T_6
1	In (1.)–290 (0.60)	In (1.)–320 (0.57)	In (1.)–320 (iso)	In (1.)–320 (0.63)
2	290 (0.59)–295 (0.56)	320 (0.58)–330 (iso)	320 (0.33)–310 (iso)	320 (0.63)–330 (0.57)
3	295 (0.57)–300 (0.53)	330 (0.33)–325 (iso)	320 (0.33)–300 (0.53)	330 (0.57)–340 (iso)
4	300 (0.53)–305 (0.48)	325 (0.33)–320 (0.57)	300 (0.52)–280 (0.64)	330 (0.57)–320 (0.63)
5	305 (0.49)–310 (iso)	320 (0.57)–325 (0.53)	300 (0.52)–295 (0.56)	320 (0.63)–310 (0.66)
6	310 (0.33)–305 (iso)	320 (0.57)–330 (iso)	300 (0.52)–305 (iso)	320 (0.63)–325 (0.61)
7	310 (0.33)–300 (0.53)		280 (0.64)–270 (0.68)	340 (0.33)–330 (0.57)
8	310 (0.33)–290 (0.60)		295 (0.54)–290 (0.59)	340 (0.33)–335 (iso)
9			305 (0.37)–300 (0.53)	

monomers), while those of systems T_b and T_6 are substantially higher. In other words, the transition temperature is practically unchanged when the three rigid cores are linked in sequence by conformationally unrestricted links, while including the bending potential E_τ increases the transition temperature by approximately 20 K. Adding to E_τ the potential E_φ has opposite effects in systems T_5 and T_6, since the transition temperature decreases 20 K in system T_5 and increases 10 K in system T_6 with respect to system T_b. This indicates that the nematic phase is favored by inclusion of E_φ when $n = 6$, while it is disfavored when $n = 5$. Considering Figure 3b, the transition temperature is expected to oscillate with increasing n, being higher when n is even and lower when n is odd. However, since the differences between curves for odd and even n become progressively less prominent in Figure 3b, these odd–even oscillation effects will tend to be less and less pronounced with increasing length of the spacers. In conclusion, the higher average transition temperature of the model trimers with respect to the monomers is mainly explained by E_τ, while the odd–even oscillations are related to the different characteristics of E_φ for odd and even spacers. Of course, the exact entity of these oscillations (i.e., the difference of transition temperature between consecutive members of the series) also depends on the other parameters of the simulations, such as density and A. It is possible that larger oscillations would be observed if the latter are regulated such that the transition temperatures are higher.

Orientational Order in the Nematic Liquids

At variance with the cylindrically symmetric entities usually simulated in the literature, the model trimers are complex entities characterized by a distribution of conformations with widely different molecular shapes. In order to provide a good alignment of the rigid cores along the director axis, different shapes have to be differently oriented in space in the nematic phase. Therefore, a complete description of the order in the nematic liquids should take simultaneously into account orientation and conformation of the trimers, which is not an easy task. A simplified, but less complete description can be given if orientational and conformational order are individually considered. This subsection illustrates the orientational distributions of the rigid cores and of the intermediate links representing the spacers, averaged over the distribution of trimer conformations in the nematic liquids.

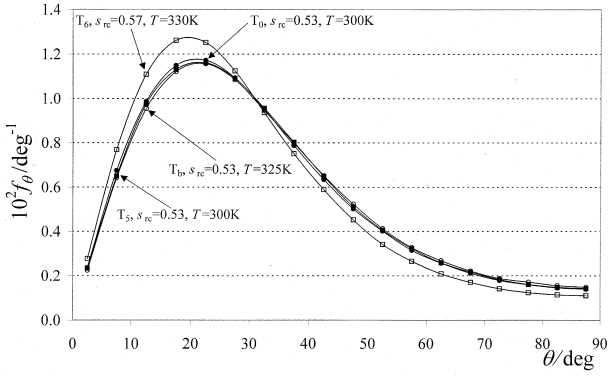

Figure 5. Orientational distribution of the rigid cores with respect to the nematic director for the nematic phase of the simulated systems at temperatures close to the isotropic–nematic transition.

Figure 5 shows the orientational distribution of the rigid cores with respect to the nematic director (the z axis) for the nematic phases at temperatures close to the transition points. Considering the curves for systems T_0, T_b and T_5, it is clear that the orientational distributions are practically coincident for a given value of s_{rc} (the slightly different curve for system T_6 is obviously related to the higher order parameter of this system). They are also remarkably identical to the curves obtained for system RC and for other systems of monomers with the same values of s_{rc}, and not far from the corresponding distributions evaluated for systems of rigid rods on the basis of the Flory–Ronca–Irvine[37, 38] and of the Mayer and Saupe[39] theories (see ref.,[35] Figure 5). Therefore, the overall nature of the order in the simulated systems appears to be scarcely affected by details of the molecular

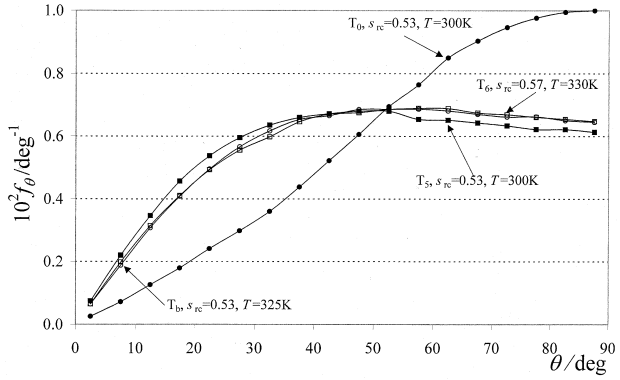

Figure 6. Orientational distribution of the links between consecutive rigid cores with respect to the nematic director for the nematic phase of the simulated systems at temperatures close to the isotropic–nematic transition.

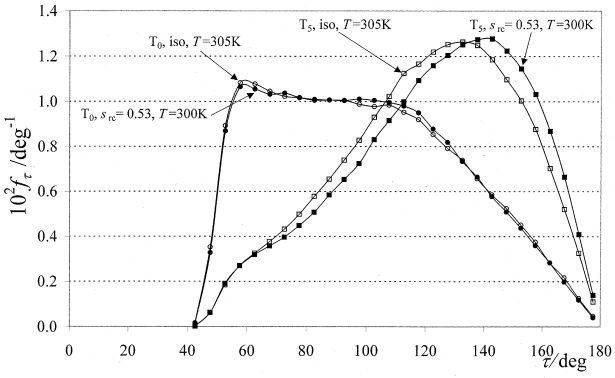

Figure 7. Distribution of the angles τ_i for systems T_0 and T_5 in the isotropic and in the anisotropic phase. The distributions for systems T_b and T_6 are very similar to those shown for system T_5.

constitution and conformation. The curves in Figure 5 are averaged over all rigid cores. It has been checked that the orientational distribution is practically the same for the central and for the external rigid cores of the trimers in all simulated systems, with the exception of system T_5, where the external cores tend to be more ordered than the central ones in the anisotropic phase. For instance, the value s_{rc} = 0.56 obtained at 295 K for system T_5 is the average of 0.57 for the external and 0.55 for the internal cores. This peculiar behavior, shown only by system T_5 (at all temperatures) among those investigated, is obviously related to the conformational distribution assumed in the nematic phase by the model trimers when E_φ is constructed to simulate $(CH_2)_n$ spacers with n odd (see below).

Figure 6 shows the orientational distribution of the links between consecutive rigid cores with respect to the z axis for the same systems examined in Figure 5. θ is defined here to be the angle between the direction of one of these links and the z axis. The distribution is not far from a $\sin\theta$ function in the case of system T_0, indicating that the links (corresponding to totally flexible spacers in this case) are practically oriented at random in this system (as shown also by the value of their order parameter along the z axis, s_{links} = −0.08). The distributions obtained for systems with the bending potential E_τ are seen to be different from that of system T_0, but very similar to each other. In other words, the orientation of the spacers depends on E_τ, while it is practically independent of E_φ. The effect of E_τ is seen to increase placements of the spacers at θ less than 50°, and to decrease those at higher angles. This is not unexpected, since on the basis of Figure 2 two rigid cores parallel to the z axis are preferentially connected by a spacer oriented at angles between 10° and 50° with respect to this axis. Anyhow, the value of s_{links} is always quite small in these systems (0.10–0.15) and the distribution is broad enough so that the spacers can be roughly considered to be disordered in the nematic phase at temperatures close to the nematic–isotropic transition. It has to be noted, however, that decreasing the temperature increases both the order parameter of the rigid cores and of the spacers (for instance, s_{rc} = 0.68 and $s_{links} \approx 0.25$ in system T_5 at 270 K).

Conformational Changes at the Nematic–Isotropic Transition

The conformational properties of the trimers in the isotropic phase near the nematic–isotropic transition point are practically what is expected on the basis of the force field adopted in the simulations, as exemplified by the distributions of τ shown in Figure 7 and by the distributions of φ shown in Figure 8a. The open symbols in Figure 7 plot f_τ curves for the isotropic phase of systems T_0 and T_5; the latter curve is typical of all trimers with the bending potential E_τ (irrespective of E_φ). The distribution is characterized, in the case of system T_0, by a broad maximum centered between 80° and 120° and by a second maximum at 60°. For system T_5, as well as for other systems with E_τ, the broad maximum is shifted at angles between 120° and 140°, while the maximum at 60° is much less intense. The two maxima at higher angles are practically as expected, while the maximum at 60° is found for all liquids of chain molecules made up of isodiametric units of this nature,[35,44] and originates from packing effects (for a discussion, see ref.[35]). Overall, the distribution of τ in the isotropic phase of trimers simulated with the bending potential E_τ is not too different from the distribution shown in Figure 2. The same is true for the distributions of φ shown in Figure 8a, in the sense that all features observed in the f_φ curves for systems T_5 and T_6 closely follow in position and intensity those present in the corresponding curves of Figure 3, while the distribution of φ is practically featureless in the case of systems T_0 and T_b. It is concluded that the conformational distribution of the

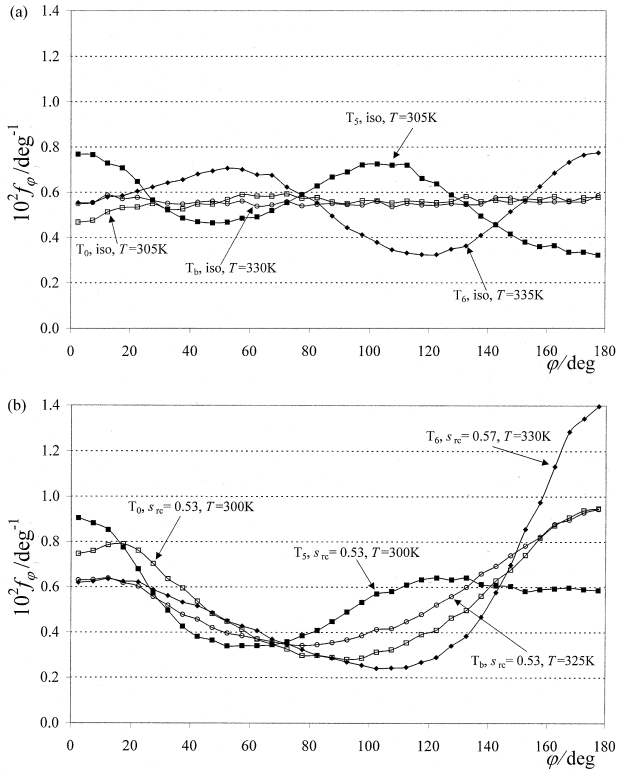

Figure 8. Distribution of the torsion angles φ_i (absolute values) for the isotropic (8a) and the nematic (8b) phase of the simulated systems at temperatures close to the isotropic–nematic transition.

model trimers is scarcely affected by packing effects in the isotropic phase, the influence being limited to a slightly higher proportion of τ angles close to 60°.

The situation is quite different in the nematic phase, where the conformational distribution is profoundly altered with respect to the isotropic liquids. In the case of system T_0, Figure 7 shows that the distributions of τ in the isotropic and in the anisotropic phase are nearly coincident, while Figure 8 shows that the uniform distribution of φ found for the isotropic liquid is changed, passing through the phase transition, in such a way that values of φ around 90° are disfavored and values close to 0° or to 180° are favored in the nematic phase. A similar behavior is shown by system T_b. However, the proportion of torsion angles in the range [0°, 60°] is smaller in system T_b than in system T_0, while that at angles ≈120° is higher. Furthermore, the distribution of τ is shifted in the nematic phase of system T_b, as well as in all other systems with the bending potential E_τ, at higher angles with respect to the isotropic phase (Figure 7). Not surprisingly, the behavior evidenced in Figure 8 for systems T_5 and T_6 is rather peculiar. In fact, torsion angles ≈120° are depleted and those ≈180° are increased in system T_6 with respect to system T_b. On the contrary, torsion angles ≈180° are depleted, and those ≈120° and ≈0° are increased in system T_5 with respect to system T_b.

The general finding that torsion angles close to 0° or to 180° are favored in the nematic phase is fairly obvious, considering that two consecutive rigid cores can be nearly parallel to the director only when $\varphi \approx 180°$ and $\tau_1 \approx \tau_2$, or when $\varphi \approx 0°$ and $\tau_1 + \tau_2 \approx 180°$. Conformations with torsion angles in the [60°, 120°] range cannot be rotated in space to have the rigid cores oriented along the director, unless τ_1 and τ_2 are both very close to 180° or to 0°. The first of these situation is quite infrequent, and the second situation is totally excluded (see Figure 7). In other words, the conformational change associated with the isotropic–nematic transition takes place in such a way to select mainly conformations with $\varphi \approx 0°$ or with $\varphi \approx 180°$, as only conformations of this kind can be rotated in space so that the rigid cores are properly oriented. It is also seen that conformations with $\varphi \approx 0°$ are less frequent in system T_b than in system T_0. This is well explained by Figure 7, considering that conformations with $\varphi \approx 0°$ can be properly aligned only when one of the two angles τ_i is less than 90°. Values of τ in this range are abundant in the case of system T_0, while they are strongly reduced in systems including E_τ. The peculiar behavior exhibited in Figure 8 for systems T_5 and T_6 can be also explained in these simple terms. In fact, conformations with $\varphi \approx 180°$ are favored by the energy contribution from the potential E_φ in system T_6, while they are disfavored in system T_5 (see Figure 3b). On the contrary, E_φ favors conformations with $\varphi \approx 0°$ in the case of system T_5, while these conformations are practically unaffected in the case of system T_6. In practice, considering $(CH_2)_n$ spacers, the conformational change associated with the transition from the isotropic to the nematic phase takes place with the assistance of E_φ for even members of the series, while it takes place in contrast to E_φ for odd members. Therefore, the transition temperature of trimers with n even is higher than the transition temperature of system T_b, while the transition temperature of trimers with n odd is lower.

It is appropriate to remark that this simplified discussion in terms of conformations with $\varphi \approx 0°$ or with $\varphi \approx 180°$ is purely schematic, given that more than 45% of the rigid cores are oriented at angles greater than 30° with respect to the director in the nematic liquids. In other words, the orientational distributions shown in Figure 5 are compatible with a much larger variety of conformational arrangements. Furthermore, conformations with $\varphi \approx 0°$ or $\varphi \approx 180°$ can be suitably oriented with respect to the nematic director only when the adjoining angles τ_1 and τ_2 are properly related (see before). This somewhat confusing situation is clarified by Figure 9, plotting the distribution of the angle α between two consecutive rigid cores for the various systems in the nematic phase at the transition points (see also ref.,[2] where $180° - \alpha$ is denoted by θ). Note that α is related to τ_1, τ_2 and φ by $\cos\alpha = \sin\tau_1 \sin\tau_2 \cos\varphi - \cos\tau_1 \cos\tau_2$. All curves in Figure 9 show two broad maxima roughly centered at $\alpha = 30°$ and at $\alpha =$

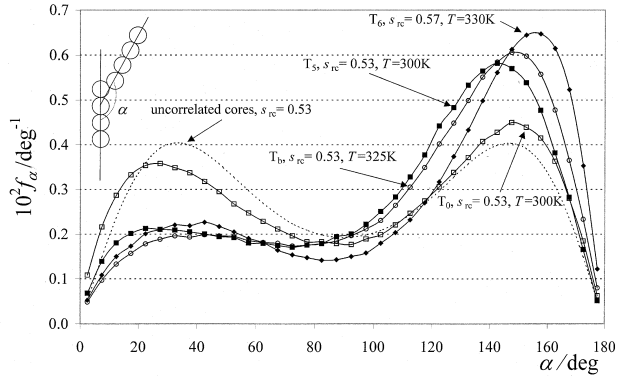

Figure 9. Distribution of the angle α between two consecutive rigid cores in a trimer molecule for the nematic phase of the simulated systems at temperatures close to the isotropic–nematic transition. The dotted curve refers to the angle between any two vectors taken at random from the orientational distribution in Figure 5 (s_{rc} = 0.53).

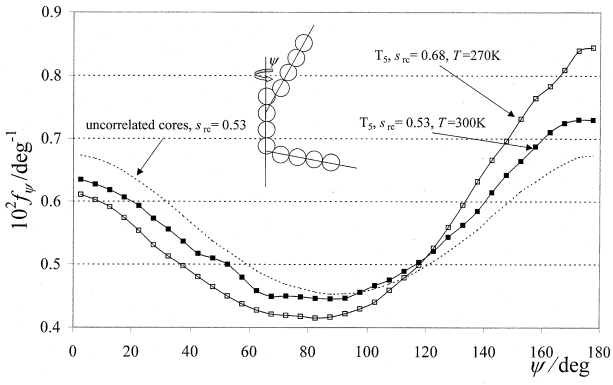

Figure 10. Distribution of the dihedral angle ψ (absolute values) defined by the directions of the three rigid cores in a trimer molecule for the nematic phase of system T_5 at 300 K and at 270 K. The dotted curve refers to the dihedral angle defined by any three vectors taken at random from the orientational distribution in Figure 5 (s_{rc} = 0.53).

150°, respectively. This is merely a consequence of the preferential orientation of the rigid cores along the director, as shown by the dotted curve, plotting the distribution of the angle between random vectors orientationally distributed as in Figure 5. The first maximum may be taken to correspond to compact conformations ($\alpha < 60°$), and the second maximum to extended conformations ($\alpha > 120°$). Within this broad definition, compact conformations are seen to be nearly as abundant as extended conformations in system T_0, while they are much less abundant in the other cases (20%, compared to 55% for extended conformations). Note that the distribution curves for the isotropic liquids show a single broad maximum, centered at 90° for system T_0 and around 120° for the other systems. This explains the reduced abundance of compact conformations in Figure 9, since these conformations are already reduced in the isotropic liquids, and is mainly related to E_τ, since adding E_φ has only minor effects. In conclusion, the conformational selection taking place at the phase transition tends to favor to an equal extent compact and extended conformations. However, for the trimers examined in this work, extended conformations are favored by E_τ. It is also found that the distribution of the angle α' between the two terminal cores of the same molecule is intermediate between the distribution of α and the dotted curve in Figure 9. In other words, the correlation between consecutive rigid cores determined by the presence of the poly(methylene) spacers is propagated through the chain and is still clearly discernible between cores separated by two intervening spacers.

The existence of long-range intramolecular correlations in the anisotropic phase is confirmed in Figure 10, plotting the distribution of the torsion angle ψ defined by the directions of the three rigid cores in a trimer molecule (note that ψ is different from φ*). The curve shown for system T_5 at 300 K is practically coincident with those for all other systems in the nematic phase at the transition point, except system T_0. In the latter system, the distribution is very similar to the dotted curve, showing the distribution of ψ for any three random vectors orientationally distributed as in Figure 5. The corresponding distributions in the isotropic phase are perfectly uniform, as expected considering that the torsion angle φ* was left completely free in all simulations. Figure 10 indicates that the phase transition is associated with a second kind of conformational selection favoring conformations with ψ near 180° and disfavoring those with ψ less than 90°. Also, the curve for system T_5 at 270 K indicates that this tendency increases with increasing s_{rc}. It is easy to check that with the two angles α near 30° or 150° (see Figure 9) the alignment of the rigid cores along the director is maximized when the three cores are in a coplanar arrangement. In particular, conformations with $\alpha_1 = \alpha_2 = 30°$ or with $\alpha_1 = \alpha_2 = 150°$ can be rotated in space such that the best possible order parameter of their rigid cores ($s_{rc,best}$) is as high as 0.91 when $\psi = 180°$; $s_{rc,best}$ is smaller for all other values of ψ, with a minimum (0.75) for $\psi = 0°$. Exactly the opposite trend is calculated for conformations with $\alpha_1 = 30°$ and $\alpha_2 = 150°$ or vice versa, since $s_{rc,best}$ is maximum when $\psi = 0°$ (0.91) and minimum when $\psi = 180°$ (0.75). One expects then that conformations with $\alpha_1 < 60°$ and $\alpha_2 < 60°$ (type A; see Figure 11) or with $\alpha_1 > 120°$ and $\alpha_2 > 120°$ (type C) be preferentially found to have $\psi > 120°$ in the nematic phase, while conformations with $\alpha_1 < 60°$ and $\alpha_2 > 120°$ or vice versa (type B) are expected to be preferentially found with $\psi < 60°$. This is fully confirmed in Table 2, where the abundance of trimer conformations is classified for various systems according to the ranges of α_1, α_2 and ψ. The data for system T_6 in the isotropic phase are obviously consistent with a uniform distribution of ψ, while those for the anisotropic phase of system T_0 show that the proportion of conformations A and C with $\psi > 120°$ is nearly twice that of the same types with $\psi < 60°$. The opposite is true

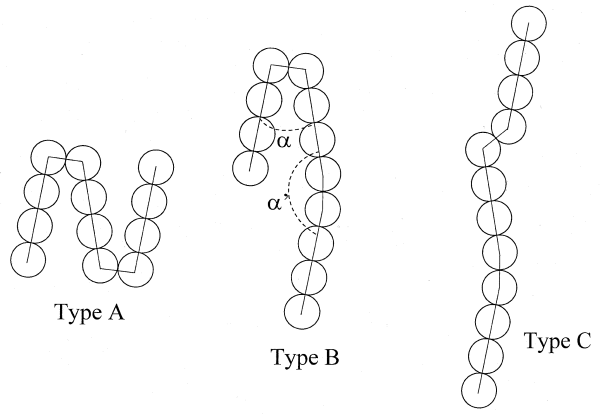

Figure 11. Conformations of Type A ($\alpha < 60^\circ$, $\alpha' < 60^\circ$; see the text), Type B ($\alpha < 60^\circ$, $\alpha' > 120^\circ$ or vice versa) and Type C ($\alpha > 120^\circ$, $\alpha' > 120^\circ$).

Table 2. Percent abundance of trimer conformations classified according to α_1, α_2 and ψ. A: $\alpha < 60^\circ$, $\alpha_2 < 60^\circ$; B: $\alpha_1 < 60^\circ$, $\alpha_2 > 120^\circ$ or vice versa; C: $\alpha_1 > 120^\circ$, $\alpha_2 > 120^\circ$.

	$\psi < 60^\circ$			$\psi > 120^\circ$		
	A	B	C	A	B	C
T_0, 300 K	2.3	13.9	3.7	6.1	7.0	8.1
T_b, 325 K	0.7	10.5	6.8	1.8	5.2	14.8
T_5, 300 K	0.9	11.6	5.5	2.3	5.3	13.4
T_6, 330 K	0.8	12.4	7.6	2.4	5.7	16.1
T_5, 270 K	0.7	15.8	7.1	2.4	5.5	24.3
T_6, iso	0.9	4.0	4.0	1.0	4.0	4.0

for conformations of type B. The same behavior is seen for the anisotropic phase of systems including E_τ, where conformations of types A and B are obviously less than in system T_0 while conformations of type C are more abundant (as dictated by the distribution of α in Figure 9). Overall, the proportion of conformations with $\psi > 120^\circ$ increases going from system T_0 to systems with E_τ. It increases even more with increasing s_{rc} (see system T_5 at 270 K), thus explaining the behavior of f_ψ in Figure 10.

Conclusions

This paper reports on the behavior of four independently simulated models of liquids of segmented-chain mesogenic trimers with a density of rigid cores comparable to that found in real systems. The trimer molecules consist of three rigid cores connected in sequence by virtual bonds representing the spacers. The four models differ for the conformational characteristics of the spacers, described in terms of a bending potential E_τ (between rigid cores and virtual bonds) and of a torsion potential E_φ (around the virtual bonds). These potentials are roughly regulated to mimic the presence of $(CH_2)_5$ and $(CH_2)_6$ spacers in system T_5 and T_6, respectively, while system T_0 corresponds to totally flexible spacers and system T_b, including only the bending potential, is utilized for comparative purposes.

In spite of the simplicity of the models and of the several approximations involved (rigid cores modeled as linear sequences of Lennard–Jones centers; anisotropic attractive forces among rigid cores modeled as a mean field; spacers modeled as structureless joints; correlations between τ and φ neglected, etc.), the thermal behavior of the simulated systems is in excellent agreement with the behavior experimentally observed for segmented-chain oligomers and polymers. In particular, all systems show reversible isotropic–nematic phase transitions at well defined temperatures characteristic of each system. In the case of system T_0, the transition temperature and the degree of order in the nematic phase are identical to those of a similar system of unconnected rigid cores, showing that totally flexible spacers behave in practice as a bound solvent. The transition temperature is higher in system T_b, due to the stiffening of the trimer molecules induced by E_τ, while adding the torsion potential E_φ has opposite effects in systems T_5 and T_6, since the transition temperature decreases for system T_5 and increases for system T_6 with respect to system T_b. Considering the behavior of E_τ and E_φ for the various members of the $(CH_2)_n$ series, the transition temperature is expected to oscillate with increasing n, being higher for n even and lower for n odd. Of course, the results described here are strictly valid for those trimers that have been simulated, in the sense that modifying E_τ and E_φ in order to model a given polymer could change not only the numerical values, but also the direction of the odd–even oscillations. However, these results show that simple models of this kind are well suited for investigating the essential aspects of thermal behavior, orientation and conformation of segmented-chain mesogenic polymers in the isotropic and in the anisotropic liquids.

The distributions of τ and φ in the isotropic liquids are in practice as expected in all cases. In particular, the distribution of φ is nearly uniform for systems T_0 and T_b. This can not be true for the nematic liquids, since the preferential orientation of the rigid cores parallel to a common direction implies that the distribution of the torsion angle around any link connecting any two rigid cores (belonging to the same trimer molecule or not) be characterized by a preponderance of values close to 0° or 180°. Therefore, the isotropic–nematic transition is coupled with a conformational selection disfavoring torsion angles around the virtual bonds (representing the spacers) in the $[60^\circ, 120^\circ]$ range and favoring those near 0° or 180°. This explains the behavior of the transition temperatures, since the transition takes place with the assistance of E_φ for even members of the series, while it takes place in contrast to E_φ for odd members.

The conformational selection is also manifested in the distribution of the angle α between two consecutive rigid cores in the same molecule. The distribution for the isotropic liquids shows a single broad maximum, centered at

90° in system T_0 and near 120° in systems with E_τ. As expected for rigid cores preferentially aligned to a common direction, the distribution for system T_0 in the nematic liquid is characterized by two nearly equivalent maxima centered at α_{max} and at $180°-\alpha_{max}$ ($\alpha_{max} \approx 30°$ for system T_0 at a temperature close to the transition point; the maxima are obviously expected to shift closer to 0° and to 180° with increasing the order parameter of the rigid cores). The situation is different for the other systems, where the second maximum is much higher than the first. Therefore, extended conformations ($\alpha > 120°$) are preferred over compact conformations ($\alpha < 60°$) for systems T_b, T_5 and T_6 in the nematic phase. This is rather obvious, since compact conformations are already reduced in the isotropic liquids. The results of the present simulations are seen to be in excellent agreement with the RIS calculations of Abe[2] and of Yoon and Bruckner,[4] highlighting the role of extended conformations for the stabilization of liquid-crystalline order in segmented-chain polymers. On the other hand, the preference for extended conformations observed in the simulated systems of trimers (except T_0) is closely related to E_τ, since approximately the same distribution is found for all systems including E_τ, while adding E_φ has only minor effects. Considering that E_τ may depend on the detailed geometry at the junction between spacers and rigid cores, there is no apparent reason for excluding that compact conformations may play a more substantial role in real systems, especially in cases in which the X–Y bonds (Figure 1) are far from being collinear with the rigid cores.

The conformational selection taking place at the isotropic–nematic phase transitions is not limited to consecutive rigid cores, but is also extended to rigid cores separated by two intervening spacers. This is shown by the fact that the distribution of the angle α' between terminal rigid cores of the trimer molecules is not symmetric for systems including E_τ, in the sense that conformations with $\alpha' > 120°$ are more abundant than conformations with $\alpha' < 60°$. It is also shown by the distribution of the dihedral angle ψ defined by the directions of the three rigid cores in a trimer molecule, since conformations with ψ near 180° are more abundant than conformations with ψ near 0°. Both effects are mainly related to the presence of E_τ, and are approximately independent from the exact form of E_φ.

Having proved that calculations of this kind are feasible, and that the simulated systems may show a thermal behavior similar to experiments at least from a qualitative point of view, the next step is obviously to study the possibility of regulating the various parameter in order to model more closely real segmented-chain polymers. In particular, the axial ratio of the rigid cores and/or the strength of the mean field can be adjusted such to give the experimental transition temperature for the monomers of a given series, while E_τ and E_φ can be obtained from single-chain calculations analogous to those performed in this paper (correlations between τ and φ should be properly included). On the other hand, the overall density of the systems (and the strength of the mean field) should be regulated to experimental values for each member of the series under study, taking into account that increasing the length of the spacers dilutes the rigid cores. Hopefully, semirealistic simulations of this kind may enhance our presently imperfect understanding of these fascinating materials.

Supplementary Material

Coordinate files of configurations of system T_5 at 300 K ($s_{rc} = 0.53$) and of system T_6 at 330 K ($s_{rc} = 0.57$) are available for downloading at URL http://micvac.dichi.unina.it.

Acknowledgement: The financial support of the Ministero dell'Università e della Ricerca Scientifica of Italy is gratefully acknowledged.

Received: January 25, 2002
Revised: March 27, 2002
Accepted: April 19, 2002

[1] [1a] A. Sirigu, in: *Liquid Crystallinity in Polymers*, A. Ciferri, Ed., VCH Publishers, Inc., New York 1991; [1b] A. M. Donald, A. H. Windle, *Liquid Crystalline Polymers*, Cambridge University Press, Cambridge 1992.
[2] A. Abe, *Macromolecules* **1984**, *17*, 2280.
[3] [3a] D. Y. Yoon, S. Bruckner, W. Wolksen, J. C. Scott, A. C. Griffin, *Faraday Discuss. Chem. Soc.* **1985**, *79*, 41; [3b] G. Sigaud, D. Y. Yoon, A. C. Griffin, *Macromolecules* **1983**, *16*, 975.
[4] D. Y. Yoon, S. Bruckner, *Macromolecules* **1985**, *18*, 651.
[5] P. J. Flory, *Adv. Polym. Sci.* **1984**, *59*, 1.
[6] [6a] P. J. Flory, *Mat. Res. Soc. Symp. Proc.* **1989**, *134*, 3; [6b] D. Y. Yoon, P. J. Flory, *Mat. Res. Soc. Symp. Proc.* **1989**, *134*, 11.
[7] D. J. Photinos, E. T. Samulski, H. Toriumi, *J. Chem. Soc., Faraday Trans.* **1992**, *88*, 1875.
[8] K. Nicklas, P. Bopp, J. Brickmann, *J. Chem. Phys.* **1994**, *101*, 3157.
[9] A. Ferrarini, G. R. Luckurst, P. L. Nordio, S. J. Roskilly, *Mol. Phys.* **1995**, *85*, 131.
[10] H. S. Serpi, D. J. Photinos, *J. Chem. Phys.* **1996**, *105*, 1718.
[11] A. Ferrarini, G. R. Luckurst, P. L. Nordio, S. J. Roskilly, *Liq. Cryst.* **1996**, *21*, 373.
[12] J. W. Emsley, G. R. Luckurst, G. N. Shilstone, *Mol. Phys.* **1984**, *53*, 1023.
[13] J. A. Ratto, F. Volino, R. B. Blumstein, *Macromolecules* **1991**, *24*, 2862.
[14] [14a] C. T. Imrie, F. E. Karasz, G. S. Attard, *Macromolecules* **1993**, *26*, 545; [14b] C. T. Imrie, F. E. Karasz, G. S. Attard, *Macromolecules* **1993**, *26*, 2803.

[15] G. Kothe, K. Müller, in: *The Molecular Dynamics of Liquid Crystals,* G. R. Luckurst, C. A. Veracini, Eds., Kluwer, Dordrecht 1994.
[16] N. J. Heaton, G. Kothe, *J. Chem. Phys.* **1998**, *108*, 8199.
[17] J. Cheng, Y. Yoon, R. Ho, M. Leland, M. Guo, S. Z. D. Cheng, P. Chu, V. Percec, *Macromolecules* **1997**, *30*, 4688.
[18] D. Frenkel, H. N. W. Lekkerkerker, A. Stroobants, *Nature* **1988**, *332*, 822.
[19] D. Frenkel, *Mol. Phys*. **1987**, *60*, 1.
[20] M. P. Allen, D. Frenkel, J. Talbot, *Comput. Phys. Rep.* **1989**, *9*, 301.
[21] D. Frenkel, *Liq. Cryst.* **1989**, *5*, 929.
[22] P. J. Camp, M. P. Allen, A. J. Masters, *J. Chem. Phys.* **1999**, *111*, 9871.
[23] M. P. Allen, *J. Chem. Phys.* **2000**, *112*, 5447.
[24] G. R. Luckurst, R. A. Stephens, R. W. Phippen, *Liq. Cryst.* **1990**, *8*, 451.
[25] M. P. Neal, M. D. De Luca, C. M. Care, *Mol. Simul.* **1995**, *14*, 245.
[26] R. Berardi, H. G. Kuball, R. Memmer, C, Zannoni, *J. Chem. Soc., Faraday Trans.* **1998**, *94*, 1229.
[27] J. G. Gay, B. J. Berne, *J. Chem. Phys.* **1981**, *74*, 3316.
[28] S. J. Picken, W. F. Van Gunsteren, P. P. Van Duijnen, W. H. De Jeu, *Liq. Cryst.* **1989**, *6*, 357.
[29] M. R. Wilson, M. P. Allen, *Liq. Cryst.* **1992**, *12*, 157.
[30] S. S. Patnaik, S. J. Plimpton, R. Pachter, W. W. Adams, *Liq. Cryst.* **1995**, *19*, 213.
[31] M. Yoneka, Y. Iwakabe, *Liq. Cryst.* **1995**, *18*, 45.
[32] Z. Wang, J. A. Lupo, S. Patnaik, R. Pachter, *Comput. Theor. Polym. Sci.* **2001**, *11*, 375.
[33] M. Vacatello, M. Iovino, *J. Chem. Phys.* **1995**, *104*, 2721.
[34] M. Vacatello, M. Iovino, *Liq. Cryst.* **1997**, *22*, 75.
[35] M. Vacatello, G. Di Landa, *Macromol. Theory Simul.* **1999**, *8*, 85.
[36] M. Vacatello, *Polym. Mat. Sci. Eng.* **2001**, *85*, 442.
[37] [37a] P. J. Flory, G. Ronca, *Mol. Cryst. Liq. Cryst.* **1979**, *54*, 289; [37b] P. J. Flory, G. Ronca, *Mol. Cryst. Liq. Cryst.* **1979**, *54*, 311.
[38] [38a] P. A. Irvine, P. J. Flory, *J. Chem. Soc., Faraday Trans.* **1984**, *80*, 1807; [38b] P. A. Irvine, P. J. Flory, *J. Chem. Soc., Faraday Trans.* **1984**, *80*, 1821.
[39] W. Maier, A. Saupe, *Z. Naturforschg*. **1959**, *14a*, 882.
[40] M. Vacatello, D. Y. Yoon, B. C. Laskowski, *J. Chem. Phys.* **1990**, *93*, 779.
[41] U. W. Suter, E. Saiz, P. J. Flory, *Macromolecules* **1983**, *16*, 1317.
[42] W. R. Krigbaum, J. Watanabe, *Polymer* **1983**, *24*, 1299.
[43] C. K. Ober, J. I. Jin, R. W. Lenz, *Polym. J.* **1982**, *14*, 9.
[44] M. Vacatello, *Macromol. Theory Simul.* **2001**, *10*, 187.